

1-22-2021

Deformation and fracturing characteristics of fracture network model and influence of filling based on 3D printing and DIC technologies

Ke ZHANG

Faculty of Electric Power Engineering, Kunming University of Science and Technology, Kunming, Yunnan 650500, China

Fei-fei QI

Faculty of Electric Power Engineering, Kunming University of Science and Technology, Kunming, Yunnan 650500, China

Yu-long CHEN

School of Energy and Mining Engineering, China University of Mining and Technology (Beijing), Beijing 100083, China

Follow this and additional works at: <https://rocksoilmech.researchcommons.org/journal>



Part of the [Geotechnical Engineering Commons](#)

Custom Citation

ZHANG Ke, QI Fei-fei, CHEN Yu-long, . Deformation and fracturing characteristics of fracture network model and influence of filling based on 3D printing and DIC technologies[J]. Rock and Soil Mechanics, 2020, 41(8): 2555-2563.

This Article is brought to you for free and open access by Rock and Soil Mechanics. It has been accepted for inclusion in Rock and Soil Mechanics by an authorized editor of Rock and Soil Mechanics.

Deformation and fracturing characteristics of fracture network model and influence of filling based on 3D printing and DIC technologies

ZHANG Ke¹, QI Fei-fei¹, CHEN Yu-long²

1. Faculty of Electric Power Engineering, Kunming University of Science and Technology, Kunming, Yunnan 650500, China

2. School of Energy and Mining Engineering, China University of Mining and Technology (Beijing), Beijing 100083, China

Abstract: Due to the complexity of fracture distribution in engineering rock mass, the physical modeling of fracture network is one of the key problems in rock mechanics experiments. In this study, a 3D printing method of fracture network model based on water-soluble materials with polyactic acid materials as supporting base is proposed. Based on the water solubility of printing material, a method for preparing rock-like model specimens containing fracture network is established. Through digital image correlation (DIC) method, the deformation and fracturing characteristics of rock-like model specimens during loading process are quantitatively studied, and the influence law of filling material is further analyzed. The experimental results show that 3D printing technology is capable to prepare complex fracture network model with satisfied repeatability of mechanical properties. The stress-strain curve of fracture network rock-like model presents several evident stress reductions before its peak strength, whereas the plastic strain softening is encountered after peak strength. DIC technology can capture the global strain field of fracture network rock-like model during the whole loading process. Moreover, the progressive evolution of strain localization is observed in the process of deformation and fracturing, which reflects the law of crack initiation, propagation and coalescence. The mechanical parameters and strain field distributions of model specimens are influenced by different filling conditions. The advantage of the proposed method is reflected by the fact that the filling material can be filled into the fractures in accordance with the actual engineering condition.

Keywords: rock mechanics; fracture network; 3D printing; fracturing; digital image correlation method; strain field

1 Introduction

Rock mass, as an engineering medium, has been widely encountered in the fields of water conservancy, civil engineering, mining and transportation. Due to the complexity of geological environment during diagenesis, a large number of structural planes are distributed inevitably and randomly in rock masses. This fracture network significantly affects the strength and stability of engineering rock masses^[1]. Therefore, the research on the deformation and fracturing mechanism of fractured rock mass has important theoretical significance and engineering value.

The physical and mechanical properties of fracture network have been studied by many scholars. Chen et al.^[2] and Yang et al.^[3] used Monte Carlo method to generate a numerical model of fracture network, and to analyze the macroscopic mechanical parameters of fractured rock mass by combining with the finite element method. Zhang et al.^[4] set a measuring line for the numerical model of random fracture network, and analyzed the scale effect and space effect of rock mass quality index. Wang et al.^[5] developed a grouting model of random fracture network and used discrete element software to simulate the diffusion process of slurry in fracture network. Limited by the complexity of specimen preparation of fracture network physical model, current

research mainly focuses on theoretical analysis. However, the corresponding laboratory tests are rarely reported.

In recent years, 3D printing technology has gradually gained the attention and applications by scholars in the field of rock mechanics due to its ability to clone 3D solid models containing complex structures^[6], which also provides a feasible approach to solve these problems. Jiang et al.^[7] attempted to print specimens with Polylactic acid (PLA) material and found that this material was not suitable for directly simulating rock materials. Ju et al.^[8] combined CT imaging and 3D printing technology to print coal and rock models using photosensitive resin materials. Liu et al.^[9] and Jiang et al.^[10] chose powder gypsum as base material of 3D printing to produce model specimens containing pores and fractures. The above studies have revealed that 3D printing technology can easily reconstruct the internal structure of rock mass, but the mechanical properties of materials such as PLA, resin and gypsum selected at present are distinct from those natural rocks^[6]. Therefore, Wang et al.^[11] printed the fracture network with PLA as raw material, and then used cement mortar closer to the rock to cast the rock mass similarity model. However, the PLA material placed in cement mortar is a plastic material with high strength and ductility^[6], so it can not accurately simulate the filling material inside the natural cracks, which have a great impact on the mechanical

Received: 19 September 2019

Revised: 26 December 2019

This work was supported by the National Natural Science Foundation of China (41762021, 11902128) and the Applied Basic Research Foundation of Yunnan Province (2019FI012)

First author: ZHANG Ke, male, born in 1986, PhD, Associate professor, Doctoral supervisor, mainly engaged in rock mechanics and engineering teaching and research work. E-mail: zhangke_csu@163.com

behavior of model specimens.

Digital image correlation (DIC) method developed in recent years has made full-field deformation measurement of specimen surface a reality, which has been paid great attention and applied in the field of rock mechanics test^[12–13]. Based on DIC method, a new laboratory test method for physical reconstruction and mechanical properties of fracture network model is proposed in this study. The fracture network model is printed with water-soluble materials, and is prepared with high strength cement mortar and low strength gypsum. Combined with DIC method, the deformation and fracturing processes of rock-like model specimen containing fracture network under compression stress are quantitatively studied. The research results provide certain references for the application and popularization of 3D printing and DIC technology in the field of rock mechanics.

2 3D printing and preparation of fracture network model

2.1 Methodology

In this study, water-soluble materials are used to print the solid fracture network model, after that the model specimen is poured by high-strength white cement mortar since the water-soluble materials are insoluble in alkaline solution at room temperature. After curing, the specimen is put into clean water to soften and remove water-soluble materials to form a rock-like model specimen with open fracture network. Finally, different strengths and types of fracture fillings are filled in according to the site investigation of the engineering rock mass.

2.2 Reconstruction of 3D digital model of fracture network

The dam foundation rock mass of a hydropower station located in the upper reaches of Lancang River in southwest China^[14] was taken as the research prototype. According to the dam section geological catalog, borehole imaging and core data, a total of 169 fractures were recorded. The corresponding fracture network in-situ model image^[14] is shown in Fig. 1(a). The square in the in-situ model (25 m×25 m, as shown in the dotted line) was selected as the study area. The study area was scaled down at a scale of 250:1 to obtain

an indoor similar model of the fracture network with a size of 100 mm×100 mm (length×width), as shown in Fig. 1(b). On this basis, the fracture network model 3D printing and rock-like model specimen preparation were carried out, and the deformation and fracturing characteristics of model specimen were studied.

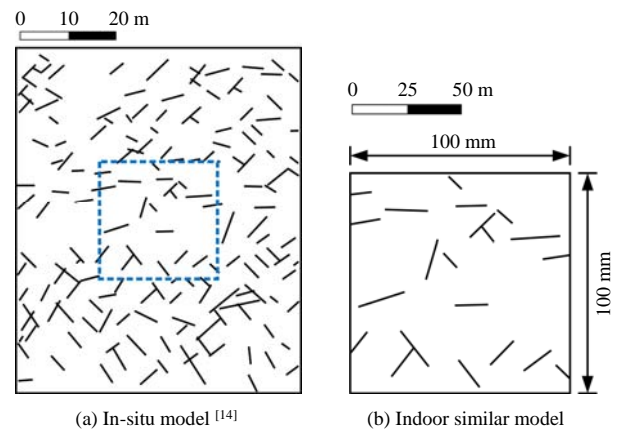


Fig. 1 Fracture network model

The reconstruction of 3D digital model of fracture network is shown in Fig. 2:

(1) The indoor similar model of fracture network (Fig. 1(b)) is identified and widened by AutoCAD, and the boundary of the model is outlined. Because the width of the fracture would affect the mechanical properties of the specimen, the width of the fracture is uniformly set at 1.2 mm. Then, using “Region” command in the software to generate the fracture network plane domain and the outer interface domain respectively, so as to obtain the 2D digital model of the fracture network.

(2) Use “Extrude” command in AutoCAD software to stretch the fracture network domain in the positive direction of Z-axis by 25 mm. The outer interface domain of the model is stretched by 0.8 mm in the negative direction of the Z-axis to generate the base model for fixing the fracture network. Then combine the above two 3D models to generate the 3D digital model of fracture network.

(3) Output the above 3D digital model into a *.stl format file, and import it into 3D printing software XYZware to obtain 3D printing digital model.

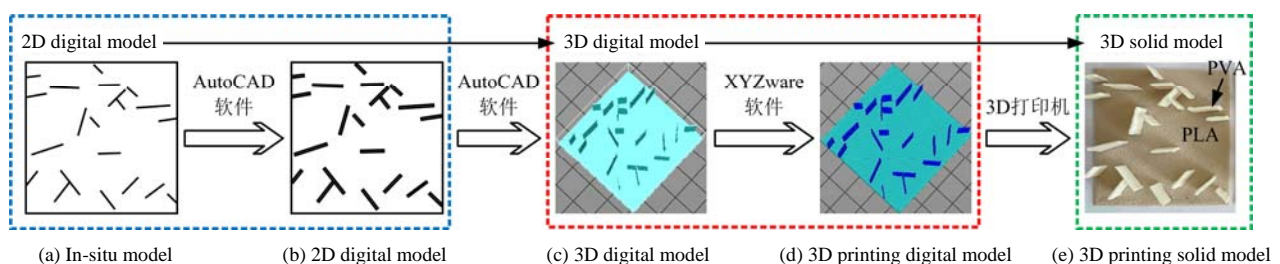


Fig. 2 Fracture network model construction and 3D printing procedure

2.3 3D printing of fracture network model

The 3D printer used in this study is Da Vinci 2.0 A Duo produced by XYZprinting, as shown in Fig. 3. It is equipped with two nozzles, diameter of which is 0.4 mm. The printing precision is 0.1mm with the maximum molding size of 200 mm×200 mm×150 mm (length×width×thickness). The consumables are polylacticacid (PLA), acrylonitrile-butadiene-styrene (ABS) and polyvinyl alcohol (PVA, a commonly used water-soluble polymer). PVA and PLA are used for 3D printing and the printing method is melt stacking method in our study. The relevant printing parameters are set as follows:



Fig. 3 Da Vinci 2.0 A Duo 3D printing system

(1) Distance between nozzle and platform (Z-axis value). Considering the thickness of 2 consumables, the Z-axis value of 3D printing is set as 1.5 mm after testing.

(2) Nozzle loading material. Place PVA and PLA into the printer respectively and choose “LOAD FILAMENT” command. A small amount of plastic drops from the nozzle, indicating that the consumable material has been successfully loaded. Nozzle 1 loads PLA material and prints the model base; Nozzle 2 loads PVA material and prints the fracture network.

(3) Nozzle and platform temperature setting. According to the properties of consumables, the 3D printer automatically matches the nozzle and platform temperature at 200° C and 50° C, respectively, so that it ensures the PLA material and PVA material have superior melting fluidity and formability.

(4) Printing accuracy setting. Considering the model printing time and accuracy comprehensively, the printing accuracy is set as 0.3 mm.

(5) Filling mode and filling rate. Fernandez-vicente et al.^[15] found that the filling mode had very little impact on the mechanical properties of the printed specimens^[15], thus the default interleaving filling method of 3D printer is adopted, and the filling rate is set to the maximum value, 90%.

The specific steps of 3D printing are as follows:

(1) Before printing, PVP solid glue is evenly applied to the printing platform according to the printing area of the fracture network model to prevent the base from becoming curved.

(2) Import the 3D printing digital model file into XYZware and set the above printing parameters; then, save it as *.3W file and execute the print command directly. The printing time of a single fracture network solid model is about 4 hours.

(3) When the printing is completed, a special shovel is used to separate the solid model of fracture network from the printing platform to finish the 3D printing.

2.4 Preparation of fracture network rock-like model specimen

After the 3D printing of the solid fracture network model, rock-like model specimen containing fracture network can be prepared. The specific operation processes are as follows (Fig. 4):

(1) The 3D printed solid model is placed in a steel mold with an internal dimension of 100 mm×100 mm×20 mm (length×width×thickness).

(2) Cement mortar is a kind of rock-like material with stable mechanical properties and superb brittleness, which is often used to simulate real rocks^[16]. In this test, high strength white Portland cement, quartz sand and water are fully stirred according to a mass ratio of 1:2:0.5, and then poured into the steel mold. The mold is then fully oscillated so that the cement mortar uniformly fills the mold.

(3) After 48 hours of pouring, the mold is removed and put into a concrete curing box for 12 days according to the standard curing method. Then soak it in clean water for 48 hours to dissolve the PVA fracture network. Finally, use tweezers to remove the residual PVA material.

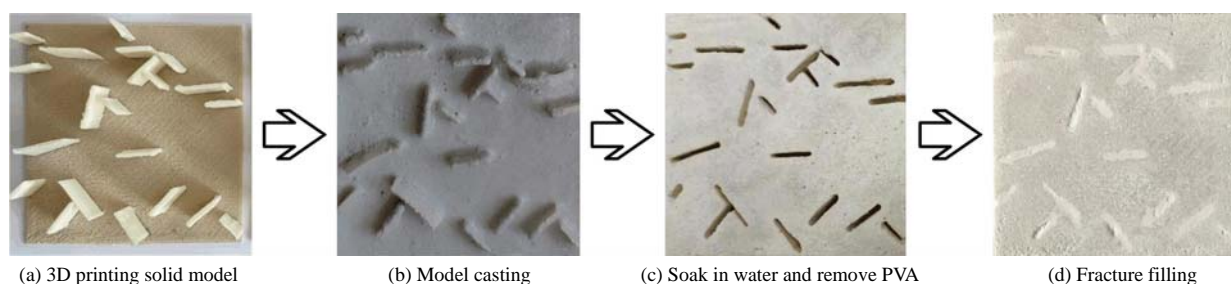


Fig. 4 Preparation procedure of rock-like model specimen containing fracture network

(4) The specimen is placed in indoor environment for 48 hours, after that its upper and lower surfaces are polished to be smooth and flat. Next, the low-strength gypsum is filled in the fracture network to simulate the fracture filling. Slightly vibrate the filling to ensure the compaction of the filling.

(5) The speckle field of specimen surface is prepared by spraying black and white paints. First, spray white primer on the front side of the specimen to enhance its contrast ratio. After the paint has dried, spray black paint about 30 cm in front of the specimen to ensure the black paint particles fall naturally on the white primer, forming random artificial speckles.

3 Deformation and fracturing characteristics of fracture network rock-like model

3.1 Testing equipment and scheme

The test system used in this study is shown in Fig. 5. The loading equipment adopts the WDW-100 universal testing machine produced by Ji'nan Shijin Group Co. Ltd. with the maximum axial force of 100 kN and an accuracy of 0.5%. Uniaxial compression test was carried out on the fracture network rock-like model specimen. The loading was controlled axially with a loading rate of 0.3 mm/min. The loading continued until the specimen was completely destroyed. During the test, the digital speckle image of specimen surface was collected in real time. The digital speckles image acquisition equipment adopted the industrial camera developed by Shenzhen Huagu Power Technology Co. Ltd. The image resolution is 2592 pixels × 1944 pixels and the acquisition rate is set as 1 frame /s. LED cold light is placed on the side of the industrial camera to provide a stable light source for image acquisition.

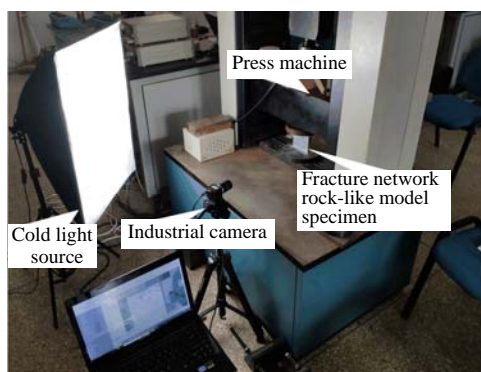


Fig. 5 Experiment system

3.2 Digital image correlation (DIC) method

The basic principles of DIC technology are illustrated in Fig. 6. Assume that the gray scale eigenvalue functions of the digital speckle image before and after the surface deformation are $I_1 = F_1(x, y)$ and $I_2 = F_2(x, y)$, respectively. Firstly, take the digital speckle image before

deformation as the reference image and select reference sub-region containing the measured point. Then search the matching target image sub-region on the digital speckle image after deformation using the correlation matching method, thereby obtaining the horizontal and vertical displacement components of the measured point, $u(x, y)$ and $v(x, y)$. The relation between the measuring point coordinates on digital speckle image before and after deformation are

$$\begin{cases} x' = x + u(x, y) \\ y' = y + v(x, y) \end{cases} \quad (1)$$

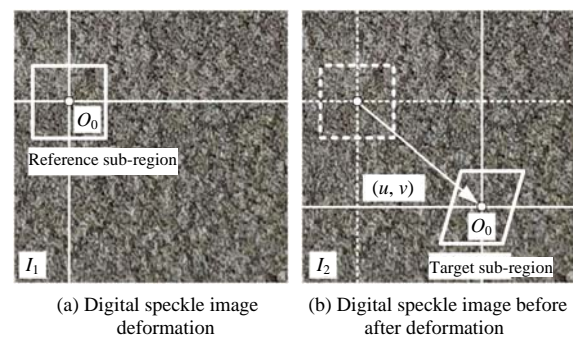


Fig. 6 Sketches of correlation match

3.3 Stress–strain curve and deformation-fracturing characteristics

Four identical low-strength rock-like model specimens containing gypsum filled fracture network are prepared, and the corresponding experimental and statistical results are list in Table 1 (elastic modulus refers to the slope of the straight line during elastic deformation stage). It can be seen that the variation coefficients of the strength and deformation parameters of these four specimens are 0.014 and 0.035, respectively, indicating that the physical and mechanical properties of the model specimens prepared by 3D printing technology are stable and have preferable repeatability.

Table 1 Experimental and statistic results of model specimens

Specimen ID	Compressive strength / MPa	Elastic modulus / GPa
1	9.070	0.970
2	9.020	0.930
3	9.220	0.980
4	8.920	0.910
Mean value	9.060	0.950
Coefficient of variation	0.014	0.035

The deformation and fracturing characteristics of all model specimens are similar, and the stress–strain curve of a typical specimen is shown in Fig. 7. Eight stress levels during loading process are marked. Table 2 shows the fracture propagation corresponding to the typical marking points a–h. The digital speckle image

collected during the whole test process was imported into digital image-related software Ncorr^[17], and the digital speckle image before loading was taken as the reference image to calculate the strain field during loading. Table 2 illustrates the horizontal strain field, vertical strain field and shear strain field corresponding to eight typical identification points. As can be seen the deformation and fracturing process of the model specimen can be roughly divided into four stages:

(1) Initial compaction (Stage I, 0–a). Similar to real rock masses, micro-fractures and micro-pores are inevitable developed in model specimens. Therefore, these primary micro-defects are gradually compacted, resulting in an up-concave stress–strain curve with significant initial nonlinear deformation characteristics. It can be seen from the strain field calculation results that the strain distribution on the surface of the specimen at point *a* is relatively uniform and the deformation is insignificant.

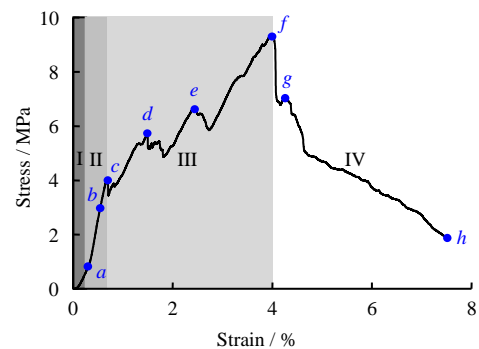
(2) Elastic deformation (Stage II, *a*–*c*). After the compaction of micro-fractures, the surfaces of the fractures contact where the friction is generated, This restrains the relative movement between the fracture surfaces and makes the axial stress and axial strain of the specimen approximately obey the linear relationship. In this stage, the strain at point *b* increases slightly, but it is still very small and is less than 8.0×10^{-4} .

(3) Fracture initiation and propagation (Stage III, *c*–*f*). When the load reaches 43.39% of the peak stress (point *c*), tensile cracks are triggered at the tip of the partially inclined fractures and the middle of the gently inclined fractures, and the axial stress drops immediately. Compared with the strain field in this stage, it can be clearly seen that a strain concentration zone appears at the point where fractures initiate and propagate around the corresponding precast fractures. Compared with intact rock and single fracture rock specimen, there are more fractures distributed in the fracture network rock-like model specimen, leading to a significant stress drop and stress fluctuation in the pre-peak phase of the stress–strain curve, which essentially reflects the continuous development of new fractures in the model specimen. Additionally, with increasing the axial load (point *d* and *e*), the interaction between the newly developed fractures and the precast fracture network becomes intensified, thus some new fractures continuously propagate, converge and connect with the prefabricated fractures; and the strain concentration zone covering the fracture propagation paths also extends and joins gradually, although a macroscopic fracture surface has not been formed. At the same time, stress equilibrium is reestablished inside the specimen.

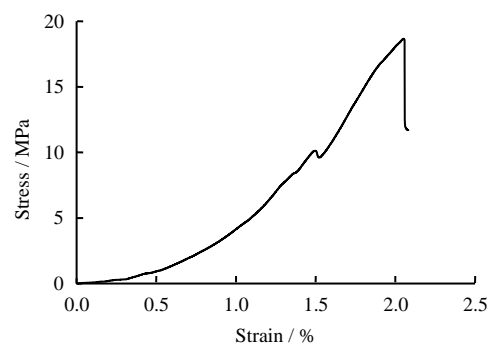
(4) Strain softening (Stage IV, *f*–*h*). When loaded to point *f*, the model specimen does not completely lose its bearing capacity. A new stress equilibrium

(points *g* and *h*) is reached after stress adjustment, showing the characteristics of plastic strain softening. In this test, we also poured the intact rock-like model specimen, and the corresponding stress–strain curve is illustrated in Fig. 6(b). It can be noted that the intact specimen shows obvious brittleness. Therefore, from the perspective of fracture propagation and transfixion, the plastic strain softening behavior of the fracture network rock-like model specimen is not the property of rock itself, and this can be attributed to the randomness, heterogeneity and anisotropy of fracture distribution, which makes it difficult to form a strain concentration zone and fracture surfaces.

To sum up, DIC technology can be used to track the global strain field and the evolution rule of strain concentration zone during the loading process of the fracture network rock-like model specimen. The strain field of the model specimen displays uniform distribution at the initial stage of loading, and then the strain concentration zone, which covers part of the precast fractures and fracture propagation paths, appear gradually. The specimen is characterized by discontinuous deformation and fracturing behaviour. Therefore, the strain concentration zone can be regarded as an important feature of fractured rock mass instability and failure, and it also reflects the law of fracture initiation, propagation and transfixion.




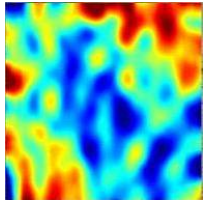
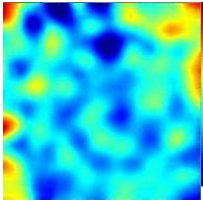
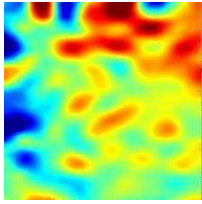

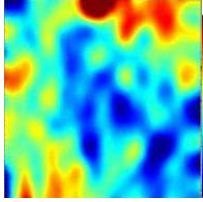
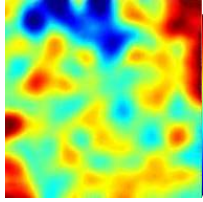
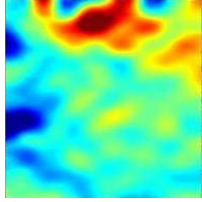

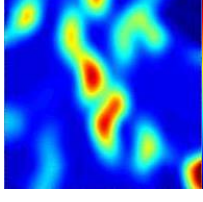
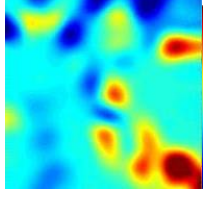
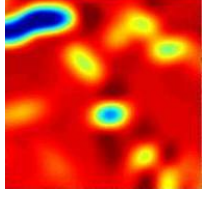

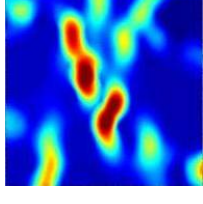
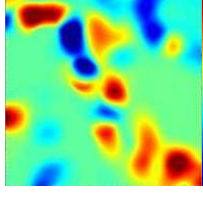
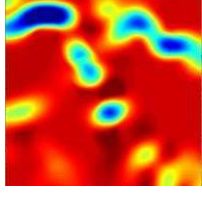

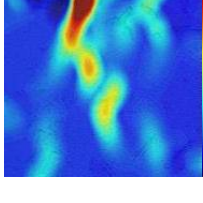
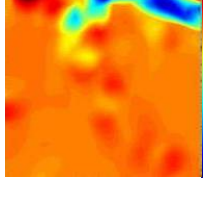
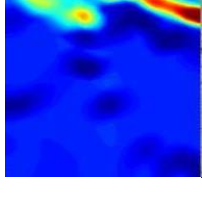
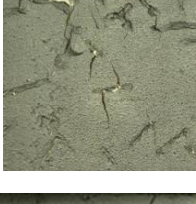
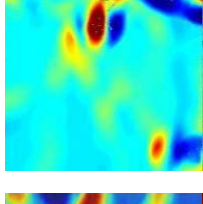
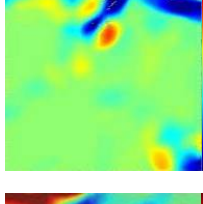
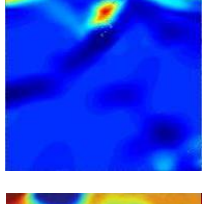
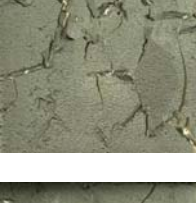
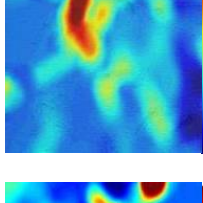
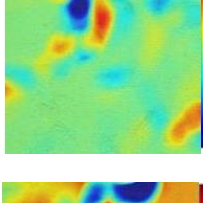
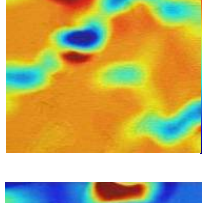

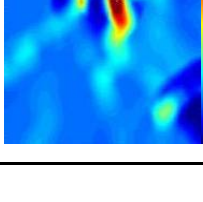
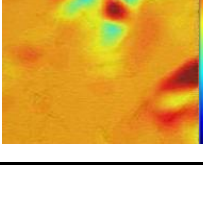
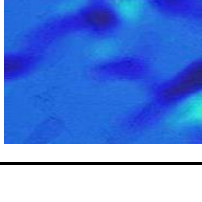
(a) Fracture network rock-like model specimen



(b) Intact rock-like model specimen

Fig. 7 Typical stress–strain curves

Table 2 Crack propagation and strain field evolution during loading process

Characteristic	Fracture propagation	Horizontal strain field	Vertical strain field	Shear strain field
<i>a</i>		 $\times 10^{-4}$	 $\times 10^{-4}$	 $\times 10^{-4}$
<i>b</i>		 $\times 10^{-4}$	 $\times 10^{-4}$	 $\times 10^{-4}$
<i>c</i>			 $\times 10^{-3}$	 $\times 10^{-3}$
<i>d</i>				
<i>e</i>				
<i>f</i>				
<i>g</i>				
<i>h</i>				

4 Influence of filling

For practical engineering rock masses, the fractures often contain ooze, gravel and other filling materials. Zhang et al.^[18] and Zhuang et al.^[19] used uniaxial compression test and numerical simulation method to compare the effect of filling on the mechanical properties of single-fracture rock specimen and fracture propagation. Yin et al.^[20] conducted uniaxial compression testing research on rock specimens with filled orthogonal fractures. From the perspective of mechanics, these fillings hold a certain bearing capacity, which will change the stress environment around the fracture to some extent, thus affecting the instability and failure of rock mass. Because of the complexity of fracture network specimen preparation, the above research mainly focuses on single fracture or double fractures. In this section, the rock-like model specimen of fracture network is taken as the research object. In addition to filling low-strength gypsum in fracture network as described in Section 3, other two filling conditions are considered: (1) Maintain PVA material; (2) After 48 hours of soaking in water, PVA material is then removed and no filling is performed after that. DIC method is used as the observation method to analyze and compare the influence of different filling conditions on deformation and fracturing characteristics of model specimen.

4.1 Mechanical parameter characteristics

Figure 8 demonstrates the stress–strain curves of the fracture network rock-like model specimen under different filling conditions.

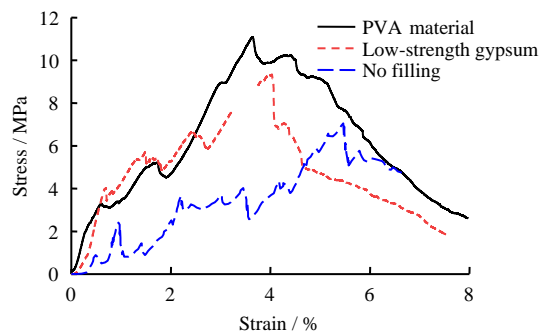


Fig. 8 Stress–strain curves under different filling conditions

It can be seen that under these three filling conditions (PVA filling, low-strength gypsum filling and no filling), the frequency and amplitude of stress–strain curves increase gradually and fluctuate considerably. Specifically, each stress plunge corresponds to an initiation of new fractures. The mechanical parameters of model specimen under different filling conditions are displayed in Table 3. Compared with the specimen without filling, the compressive strength and elastic modulus of the model specimen after filling are all enhanced although the increments are different. The compressive strength of the specimen is increased by PVA material and low-strength gypsum are 57.17%

and 30.78%, respectively, and the increase of the elastic modulus are 15.29% for these two fillings. The results highlight that the filling materials have a significant influence on the mechanical parameters of fracture network. Compared with the research of Wang et al.^[11], the model preparation method proposed in this study has remarkable advantages. Using water-soluble material as the base material for fracture network 3D printing and filling with different types and strengths materials can meet the requirements of model test of practical engineering rock masses.

Table 3 Experimental results of model specimens under different filling conditions

Filling condition	Compressive strength	Elastic modulus
	/ MPa	/ GPa
PVA material	11.08	0.98
low-strength gypsum	9.22	0.98
no filling	7.05	0.85

4.2 Characteristics of global strain field

Table 4 shows the failure modes and horizontal strain field distribution under different filling conditions when the axial strain is 0.5%. It can be seen that the presence of filling exerts an important impact on the strain field distribution at the initial loading stage. At this stage, no new fracture initiation is observed in both PVA and low-strength gypsum filled specimens, and the strain concentration of precast fractures is less obvious. The horizontal strain values are maintained at a low level of 2.7×10^{-3} and 4.5×10^{-3} , respectively. However for non-filling specimen, under the same stress level, an obvious strain concentration zone has formed around some fractures and the maximum horizontal strain value is up to 0.03. This indicates that the strain around the fractures has been improved due to the bearing capacity of the filling. Therefore, compared with the non-filling condition, the axial strain required for crack initiation after filling increases significantly. Table 5 shows the failure modes and horizontal strain field distribution under different filling conditions when the axial strain value is 7%. It can be found that the macro-fracture surfaces are roughly similar under the three filling conditions, but the strain values increase successively. The maximum horizontal strain values are 0.24, 0.28 and 0.51, respectively.

In this study, 3D printing and DIC technology are combined to conduct experimental explorations on the preparation of fractured rock mass and its deformation and fracturing rules, which will also be a hot research topic in the field of experimental rock mechanics. It should be noted that the fracture network model in this study is essentially generated by directly stretch the 2D fracture network section, which mainly describes the fracture distribution state for a typical section. The next step is to study how to prepare real 3D fracture network model specimen, so as to reflect the 3D spatial distribution of fractures in a more realistic way. In addition, the future work will take advantages of the high precision of 3D printing to prepare fractures with

different widths and analyze their effects on the mechanical properties of specimens.

Table 4 Crack propagations and horizontal strain fields at axial strain of 0.5%

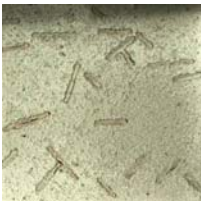
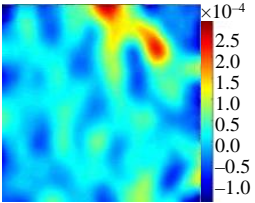

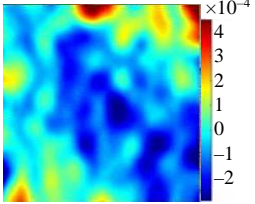

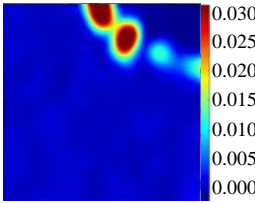
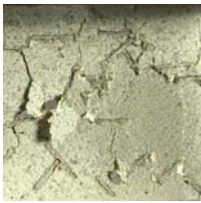
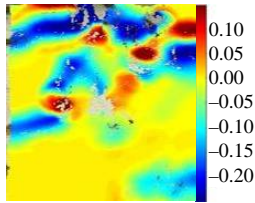

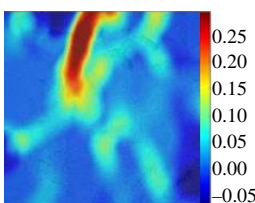

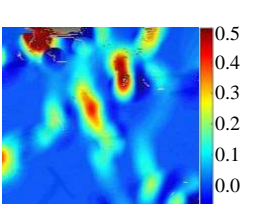
Filling conditions	Fracture propagation	Horizontal strain field
PVA material		
Low strength gypsum		
No filling		

Table 5 Crack propagations and horizontal strain fields at an axial strain of 7%

Filling conditions	Fracture propagation	Horizontal strain field
PVA material		
Low strength gypsum		
No filling		

5 Conclusions

In this paper, the combination of 3D printing and DIC technology provides a novel approach for the complex structure reconstruction and strain field quantitative analysis of fractured rock mass, which is a

promising prospect in the field of rock mechanics test.

The main conclusions are drawn as follow:

(1) In this paper, a method for modeling and preparing fracture network rock-like model based on 3D digital reconstruction and 3D printing is developed. The in-situ model of complex fracture network can be used as a reference model to make indoor similar model with high efficiency, high precision and high repeatability. The study shows that the test results of the model specimens have a small degree of deviation, indicating that it has the potential to be a reliable physical model for the analysis and comparison of the deformation and fracturing characteristics of fractured rock mass.

(2) Due to the extensive distribution of natural cracks in the rock-like fracture network model specimen, the stress-strain pre-peak curve has significantly multiple fluctuations and stress plunges along with the development of new fractures. This phenomenon is more severe than that of intact rock and single-fracture rock specimen. In the post-peak stage, the fracture is characterized by plastic strain softening, which is caused by the randomness, heterogeneity and anisotropy of fracture distribution.

(3) DIC technique realizes non-contact, full-field and full-course observation, which makes it capable to quantitatively characterize the evolution of strain field and strain concentration zone in the loading process of fracture network rock-like model specimen. This process involves a transition from uniform deformation to discontinuous deformation and failure, reflecting the processes of fracture initiation, propagation and transfixion. In short, DIC technology provides a quantitative analysis method for studying the deformation and fracturing mechanism of complex fractured rock mass.

(4) This study makes full use of the characteristics of water-soluble materials, and the prepared model specimen can be filled with corresponding fracture fillings according to the requirement of engineering rock mass model tests. The results also reveal that these fillings will affect the mechanical parameters and strain field distribution of the fracture network rock-like model specimen since the bearing capacity of filling itself changes the strain around the fractures.

References

- [1] LIU Xue-wei, LIU Quan-sheng, LIU Jian-ping, et al. Experimental study on mechanism for fracture network initiation under complex stress conditions[J]. Chinese Journal of Rock Mechanics and Engineering, 2016, 35(Suppl.2): 3662–3670.
- [2] CHEN Wei-zhong, YANG Jian-ping, ZOU Xi-de, et al. Research on macromechanical parameters of fractured rock masses[J]. Chinese Journal of Rock Mechanics and Engineering, 2008, 27(8): 1569–1574.
- [3] YANG Jian-ping, CHEN Wei-zhong, DAI Yong-hao.

- Study of scale effect of deformation modulus of fractured rock mass part I: finite element method[J]. *Rock and Soil Mechanics*, 2011, 32(5): 1538–1545.
- [4] ZHANG Wen, CHEN Jian-ping, YUAN Xiao-qing, et al. Study of size effect and spatial effect of RQD for rock masses based on three-dimensional fracture network[J]. *Chinese Journal of Rock Mechanics and Engineering*, 2012, 31(7): 1437–1445.
- [5] WANG Xiao-ling, LI Rui-jin, AO Xue-fei, et al. Three-dimensional numerical simulation of grouting in stochastic fracture network of dam bedrock in hydropower engineering[J]. *Engineering Mechanics*, 2018, 35(1): 148–159.
- [6] LIU Quan-sheng, HE Fan, DENG Peng-hai, et al. Application of 3D printing technology in physical modelling in rock mechanics[J]. *Rock and Soil Mechanics*, 2019, 40(9): 3397–3404.
- [7] JIANG C, ZHAO G. A preliminary study of 3D printing on rock mechanics[J]. *Rock Mechanics and Rock Engineering*, 2015, 48(3): 1041–1050.
- [8] JU Yang, XIE He-ping, ZHENG Ze-min, et al. Visualization of the complex structure and stress field inside rock by means of 3D printing technology[J]. *Chinese Science Bulletin*, 2014, 59(32): 3109–3119.
- [9] LIU Hua-bo, ZHAO Yi-xin, JIANG Yao-dong, et al. Experimental study of mechanical properties of 3D printing gypsum specimens[J]. *Mechanics in Engineering*, 2017, 39(5): 455–460.
- [10] JIANG Quan, SONG Lei-bo. Application and prospect of 3D printing technology to physical modeling in rock mechanics[J]. *Chinese Journal of Rock Mechanics and Engineering*, 2018, 37(1): 23–37.
- [11] WANG Pei-tao, LIU Yu, ZHANG Liang, et al. Preliminary experimental study on uniaxial compressive properties of 3D printed fractured rock models[J]. *Chinese Journal of Rock Mechanics and Engineering*, 2018, 37(2): 364–373.
- [12] MUNOZ H, TAHERI A. Specimen aspect ratio and progressive field strain development of sandstone under uniaxial compression by three-dimensional digital image correlation[J]. *Journal of Rock Mechanics and Geotechnical Engineering*, 2017, 9(4): 599–610.
- [13] JI Wei-wei, PAN Peng-zhi, MIAO Shu-ting, et al. Fracture characteristics of two types of rocks based on digital image correlation[J]. *Rock and Soil Mechanics*, 2016, 37(8): 2299–2305.
- [14] DENG Shao-hui, WANG Xiao-ling, YU Jia, et al. Simulation of grouting process in rock masses under a dam foundation characterized by a 3D fracture network[J]. *Rock Mechanics and Rock Engineering*, 2018, 51: 1801–1822.
- [15] FERNANDEZ-VICENTE M, CALLE W, FERRANDIZ S, et al. Effect of infill parameters on tensile mechanical behavior in desktop 3D printing[J]. *3D Printing and Additive Manufacturing*, 2016, 3(3): 183–192.
- [16] ZHANG Ke, LIU Xiang-hua, LI Kun, et al. Investigation on the correlation between mechanical characteristics and fracturing fractal dimension of rocks containing a hole and multi-flaws[J]. *Chinese Journal of Rock Mechanics and Engineering*, 2018, 37(12): 149–158.
- [17] BLABER J, ADAIR B, ANTONIOU A. Ncorr: open-source 2D digital image correlation Matlab software[J]. *Experimental Mechanics*, 2015, 55(6): 1105–1122.
- [18] ZHANG Bo, LI Shu-cai, ZHANG Dun-fu, et al. Uniaxial compression mechanical property test, fracture and damage analysis of similar material of jointed rock mass with filled cracks[J]. *Rock and Soil Mechanics*, 2012, 33(6): 51–56.
- [19] ZHUANG X, CHUN J, ZHU H. A comparative study on unfilled and filled crack propagation for rock-like brittle material[J]. *Theoretical and Applied Fracture Mechanics*, 2014, 72: 110–120.
- [20] YIN Qian, JING Hong-wen, SU Hai-jian, et al. Strength characteristics and crack coalescence evolution of granite specimens containing orthogonal filling fissures under uniaxial compression[J]. *Journal of China University of Mining and Technology*, 2016, 45(2): 225–232.